Contribution from the Laboratorium für Anorganische Chemie, ETH-Z, ETH Zentrum, CH-8092 Zürich, Switzerland, and Institut de chimie, Université de Neuchâtel, CH-2000 Neuchâtel, Switzerland

Kinetics and Product Distribution of the Spontaneous Cleavage of the $[(H_3N)_5CoOHCo(NH_3)_5]^{5+}$ Ion in the Presence of Competing Anions. The Question of Stepwise vs. Concerted Substitution in Spontaneous Aquation

FRANÇOIS P. ROTZINGER and WERNER MARTY*[1]

Received January 18, 1984

The spontaneous cleavage of $[(H_3N)_5CoOHCo(NH_3)_5]^{5+}$ ($=M^{5+}$) in NO_3^-/ClO_4^- and NCS^-/ClO_4^- follows the rate laws

$$k_{obsd} = \frac{k_0 + k_{NO_3}K_{NO_3}[NO_3^-]}{1 + K_{NO_3}[NO_3^-] + K_{(NO_3)_2}K_{NO_3}[NO_3^-]^2} \quad \text{and} \quad k_{obsd} = k_0/(1 + a[Y^-])$$

respectively. These rate laws are interpreted in terms of formation of reactive and unreactive ion pairs of M^{5+} with NO_3^- and NCS^-, respectively. Considerable amounts of $(H_3N)_5CoY^{2+}$ ($Y^- = NO_3^-$, *N*CS⁻, and *S*CN⁻) arise from anion scavenging by coordinatively unsaturated intermediate states in this reaction. The product distribution functions, $F([Y^-]) = [(H_3N)_5CoY^{2+}]_\infty/[M^{5+}]_0$ have been measured and are discussed in terms of alternative modes of formation; scavenging can occur either from the second coordination sphere (i.e. by intramolecular reaction within an ion aggregate with Y^-) or by intermolecular reaction of Y^- from solution. The reactive species may be the unaggregated reactant (or species aggregated with the background electrolyte anion, ClO_4^-) and/or aggregates with Y^-. Among the corresponding kinetic schemes, only the one *involving* M^{5+} *as well as* $M{\cdot}Y^{4+}$, *with* $M{\cdot}Y^{4+}$ *scavenging* Y^- *from solution and not from the second coordination sphere*, leads to the simplest model to give a satisfactory fit. The reactive intermediate states are quite selective for anions (as well as for the N terminus of NCS^-; the ratio of N/S product is ~4), and this is interpreted as arising from a genuine, coordinatively unsaturated intermediate in this spontaneous aquation process.

Introduction

Recent work on the mechanism of induced substitution on Co(III) pentaammines, such as the nitrosation of $(H_3N)_5CoN_3^{2+}$ [2-5] and the mercury-induced aquation[2,3,5] and base hydrolysis[6-8] of Co(III) halogenopentaammines, has led to controversy. Different views are held as to how nucleophiles are scavenged by coordinatively unsaturated intermediate states arising in the substitution process. The observations are consistent with dissociative activation of the leaving group, yet in some cases, the kinetics show terms dependent on $[Y^-]$.[2,5,9] While these terms give clear evidence for reactive ion aggregates with the entering nucleophile, the criteria for *concertedness* of the ligand exchange are incompletely fulfilled. Analysis of the product distribution function, $F([Y^-]) = [(H_3N)_5CoY^{2+}$(from scavenging of anions)$]_\infty/[$starting material$]_0$[2-4] showed that these reactive anion aggregates do not exclusively scavenge anions from the second coordination sphere as anticipated for concerted substitution. Discrepancies between the amounts of anionic competitor scavenged and the relative amounts of reactive ion pairs at a given competitor concentration were also noted.[2] On the other hand, the product distributions reflect the influence of the leaving group and its charge,[2-8] and this is inconsistent with a *discrete intermediate* of sufficient lifetime to equilibrate its immediate environment with the bulk solution. The Debye–Hückel ionic atmosphere of the reacting species is likely to exert its influence here.[2,6]

Spontaneous aquation has not been studied in such depth until recently. The major reason for this was that, with available leaving groups, the anion-scavenging products and the substrate were hydrolyzed at similar rates, thus obscuring the (relatively small) effective scavenging in all but very few cases. This has now been overcome by the recent synthesis of cobalt(III) pentaammines with very fast leaving groups such as $CF_3SO_3^-$,[10] ClO_4^-,[11] p-$O_2NC_6H_4SO_3^-$,[10] and FSO_3^-.[12] Anion competition proved much less effective in spontaneous aquation than in the induced aquation reactions.[10,12] For this and other reasons, it has been argued that spontaneous aquation is a concerted (I_d) rather than stepwise ligand exchange,[13] and no discrete, coordinatively unsaturated intermediate is involved.

Scheme I. Acid-Induced and Spontaneous Cleavages of the "Mono-ol" Cation

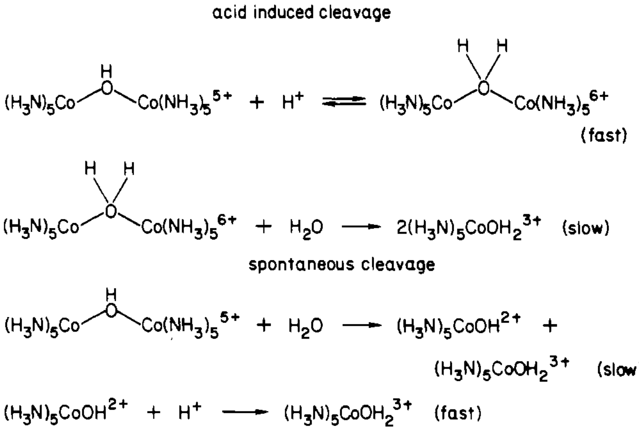

This paper deals with another case where spontaneous aquation is fast enough for straightforward anion competition studies. The "mono-ol" cation $[(H_3N)_5CoOHCo(NH_3)_5]^{5+}$ ($=M^{5+}$)[14] undergoes solvolytic cleavage by an acid-induced pathway and a spontaneous pathway (Scheme I), and both give rise to anion

---

[1] To whom correspondence should be addressed at the Université de Neuchâtel.

[2] Jackson, W. G.; Lawrance, G. A.; Sargeson, A. M. *Inorg. Chem.* **1980**, *19*, 1001.

[3] Buckingham, D. A.; Clark, C. R.; Webley, W. S. *Inorg. Chem.* **1982**, *21*, 3353.

[4] Reynolds, W. L.; Glavas, M.; Dzelilovic, E. *Inorg. Chem.* **1983**, *22*, 1946.

[5] Buckingham, D. A.; Clark, C. R.; Webley, W. S. *J. Chem. Soc., Dalton Trans.* **1980**, 2255.

[6] Dixon, N. E.; Jackson, W. G.; Marty, W.; Sargeson, A. M. *Inorg. Chem.* **1982**, *21*, 688.

[7] Jackson, W. G.; Begbie, C. M.; Randall, M. L. *Inorg. Chim. Acta* **1983**, *70*, 7.

[8] Reynolds, W. L.; Hafezi, S. *Inorg. Chem.* **1978**, *17*, 1819.

[9] Posey, F. A.; Taube, H. *J. Am. Chem. Soc.* **1957**, *79*, 255.

[10] Buckingham, D. A.; Cresswell, P. J.; Sargeson, A. M.; Jackson, W. G. *Inorg. Chem.* **1981**, *20*, 1647.

[11] Harrowfield, J. M.; Sargeson, A. M.; Singh, B.; Sullivan, J. C. *Inorg. Chem.* **1975**, *14*, 2864.

[12] Jackson, W. G.; Begbie, C. M. *Inorg. Chem.* **1981**, *20*, 1654.

[13] Swaddle, T. W. *Coord. Chem. Rev.* **1974**, *14*, 217.

[14] Siebert, H.; Feuerhake, H. *Chem. Ber.* **1969**, *102*, 2951.

0020-1669/85/1324-1617$01.50/0

Table I. Kinetics of Spontaneous Cleavage of $[(H_3N)_5CoOHCo(NH_3)_5](NO_3)_5$ in NO_3^-/ClO_4^- Media at pH 3.3 ($HClO_4$), 25.0 ± 0.1 °C, and $I = 1.0$ ($NaNO_3$, $NaClO_4$)

$[NO_3^-]$, mol dm^{-3}	10^3k_{obsd},^{a} s^{-1}	10^3k_{calcd}, s^{-1}	
		b	*c*
0.0	4.26 ± 0.06 (4)	4.42	4.26
0.02	4.31 ± 0.05 (3)	4.30	4.26
0.039	4.22 ± 0.02 (3)	4.20	4.23
0.091	4.02 ± 0.24 (3)	3.93	4.06
0.167	3.87 (1)	3.60	3.75
0.2	3.65 (1)	3.47	3.62
0.286	3.54 (1)	3.18	3.29
0.334	3.07 ± 0.17 (4)	3.04	3.13
0.445	2.78 ± 0.28 (2)	2.76	2.80
0.5	2.42 ± 0.13 (3)	2.64	2.66
0.556	2.69 ± 0.00 (2)	2.52	2.53
0.667	2.40 ± 0.41 (2)	2.33	2.31
0.715	2.12 ± 1.20 (2)	2.25	2.22
0.8	2.21 ± 0.44 (2)	2.13	2.09
0.834	2.10 ± 0.06 (4)	2.09	2.04
0.91	1.88 ± 0.19 (3)	1.99	1.94
1.00	1.72 ± 0.03 (5)	1.89	1.83

[a] Error limits for 95% confidence; number of determinations in parentheses. [b] Values calculated for rate law 1: $k_0 = 4.42 \times 10^{-3}$ s^{-1}, $a = 1.4$ dm^3 mol^{-1}. [c] Values calculated for rate law 2: $k_0 = 4.26 \times 10^{-3}$ s^{-1}, $k_{NO_3} = 4.4 \times 10^{-3}$ s^{-1}, $K_{NO_3} = 8.9$ dm^3 mol^{-1}, $K_{(NO_3)_2} = 1.6$ dm^3 mol^{-1}.

scavenging.[15] Here, kinetic and product analysis data on the spontaneous cleavage in the presence of different anions are analyzed in order to determine the intimate nature of the product-determining step.

Results

Kinetics. The spontaneous (acid-independent) cleavage of the mono-ol cation (Scheme I) occurs in the range pH 3.0–3.5 and involves substitution at only one of the two Co(III) centers.[15] We have measured the kinetics spectrophotometrically at 360 nm in NO_3^-/ClO_4^- and NO_3^-/NCS^- media at 25 °C and $I = 1.0$ ($NaClO_4$). In this wavelength range, the absorptivity of the complex increases sharply, which is detrimental to the precision. However, the salts of the mono-ol are not soluble enough to allow measurements in the vis region and possible, more distinct UV features are obscured by the absorption of the supporting electrolyte. The main problem was the very poor solubility of the starting compound. Attempted measurements in Br^-/ClO_4^- and I^-/ClO_4^- media remained unsuccessful, as insoluble salts rapidly precipitated. Also in the other mixed-electrolyte media, mixed-anion species[14] rapidly precipitated, and except where the medium contained but one anion, the kinetics were run in supersaturated solutions.[16] As a consequence, many irreproducible runs were obtained, and the data (Tables I and IIIb) have passed rigorous screening for smoothness of the curves $D_t = f(t)$ and for linearity of the $\ln |D_t - D_\infty| = f(t)$ plots for >90% of the reaction. Despite these precautions, the accuracy and precision of the present data are inferior to those of exemplary studies in the field.[17] The first-order rate law $-d[\text{mono-ol}]_{tot}/dt = k_{obsd}[\text{mono-ol}]_{tot}$ was followed, and runs in the range pH 3.0–3.5 confirmed the $[H^+]$ independence of the rates.

In NCS^-/ClO_4^- media ($[NCS^-] = 0–1$ mol dm^{-3}), the rate law

$$k_{obsd} = k_0/(1 + a[Y^-]) \qquad (1)$$

Table II. Kinetics of Spontaneous Cleavage of $[(H_3N)_5CoOHCo(NH_3)_5]Cl_5 \cdot H_2O$ in Cl^-/ClO_4^- Media at pH 3.5 ($HClO_4$), 25.0 ± 0.1 °C, and $I = 1.0$ (NaCl, $NaClO_4$)

$[Cl^-]$, mol dm^{-3}	10^3k_{obsd},^{a} s^{-1}	10^3k_{calcd}, s^{-1}	
		b	*c*
0.0	3.96	4.0	4.05
0.10	3.3	3.10	3.17
0.20	2.57	2.50	2.60
0.25	2.46	2.30	2.39
0.40	1.86	1.85	1.94
0.50	1.65	1.63	1.72
0.60	1.46	1.46	1.56
0.75	1.27	1.26	1.37
0.90	1.09	1.10	1.23
1.00	1.03	1.02	1.15

[a] Data from ref 15. [b] Values calculated for rate law 1: $k_0 = 4.0 \times 10^{-3}$ s^{-1}, $a = 2.9$ dm^3 mol^{-1}. [c] Values calculated for rate law 2: $k_0 = 4.05 \times 10^{-3}$ s^{-1}, $k_{Cl} = 3.38 \times 10^{-3}$ dm^3 mol^{-1}, $K_{Cl} = 17.1$ dm^3 mol^{-1}, $K_{Cl_2} = 2.37$ dm^3 mol^{-1}.

Table III. Kinetics of the Spontaneous Cleavage of the Mono-ol Cation in the Presence of NCS^- at 25.0 ± 0.1 °C, $I = 1.0$, and pH 3.3

(a) In NCS^-/ClO_4^- Media (NaNCS, $NaClO_4$)

$[NCS^-]$, mol dm^{-3}	10^3k_{obsd},^{a} s^{-1}	10^3k_{calcd},^{b} s^{-1}
0.0	4.39 ± 0.10 (3)	4.44
0.0476	4.25 ± 0.02 (3)	4.25
0.1	4.04 ± 0.15 (3)	4.05
0.2	3.78 ± 0.15 (3)	3.73
0.3	3.52 ± 0.05 (3)	3.45
0.4	3.22 ± 0.09 (4)	3.21
0.5	3.04 ± 0.14 (4)	3.00
0.6	2.79 ± 0.08 (4)	2.82
0.7	2.63 ± 0.06 (3)	2.66
0.8	2.48 ± 0.12 (3)	2.51
0.9	2.38 ± 0.07 (3)	2.38
1.0	2.26 ± 0.05 (3)	2.27

(b) In NO_3^-/NCS^- Media (NaNCS, $NaNO_3$), with NCS^- as the Background Electrolyte

$[NO_3^-]$, mol dm^{-3}	10^3k_{obsd},^{a} s^{-1}	10^3k_{calcd}, s^{-1}	
		c	*d*
0.0	2.26 ± 0.05 (3)	2.31	2.26
0.1	2.22 (1)	2.23	2.25
0.2	2.25 (1)	2.15	2.20
0.3	2.10 (1)	2.08	2.14
0.4	2.07 (1)	2.01	2.07
0.5	1.98 ± 0.12 (3)	1.95	2.00
0.6	1.96 (1)	1.89	1.92
0.7	1.86 ± 0.05 (4)	1.83	1.85
0.8	1.76 ± 0.08 (4)	1.78	1.78
0.9	1.73 ± 0.06 (4)	1.73	1.72
1.0	1.65 ± 0.09 (4)	1.69	1.66

[a] Limits of error for 95% confidence limits, number of determinations in parentheses. [b] Best fit to rate law 1: $k_0 = 4.44 \times 10^{-3}$ s^{-1}, $a = 0.96$ dm^3 mol^{-1}, $R = 0.009$. [c] Best fit to rate law 1: $k'_0 = 2.31 \times 10^{-3}$ s^{-1}, $a = 0.37$ dm^3 mol^{-1}, $R = 0.020$. [d] Best fit to rate law 3: $k'_0 = 2.26 \times 10^{-3}$ s^{-1}, $k'_{NO_3} = 2.31 \times 10^{-3}$ s^{-1}, $K'_{NO_3} = 2.17$ dm^3 mol^{-1}, $K'_{(NO_3)_2} = 0.56$ dm^3 mol^{-1}, $R = 0.011$.

($Y^- = NCS^-$) obtains (Table IIIa). The values of the parameters are given in Table III. This rate law corresponds to that found for Cl^-/ClO_4^- (Table II) and $CH_3SO_3^-/ClO_4^-$ media.[15] In NO_3^-/ClO_4^- media ($[NO_3^-] = 0–1$ mol dm^{-3}), rate law 1 was not equally satisfactory (Table I). Small, systematic deviations were noted at low $[NO_3^-]$, where accuracy and reproducibility were best. The curvature of the plot k_{obsd}^{-1} vs. $[Y^-]$ (calculated curve according to rate law 2) is shown in Figure 1. The data were therefore fitted to the extended rate law

$$k_{obsd} = \frac{k_0 + k_{NO_3}K_{NO_3}[NO_3^-]}{1 + K_{NO_3}[NO_3^-] + K_{(NO_3)_2}K_{NO_3}[NO_3^-]^2} \qquad (2)$$

---

(15) Buckingham, D. A.; Marty, W.; Sargeson, A. M. *Inorg. Chem.* **1974**, *13*, 2165.

(16) We find that the reproducibility of the runs was particularly poor when spectrophotometric cells with ground-glass stoppers were used. Solubility measurements on the mono-ol salts appear virtually impossible since their solvolysis is quite rapid.

(17) These problems were not encountered in the acid-induced pathway, since the observed rates are much higher and thus faster than precipitation.

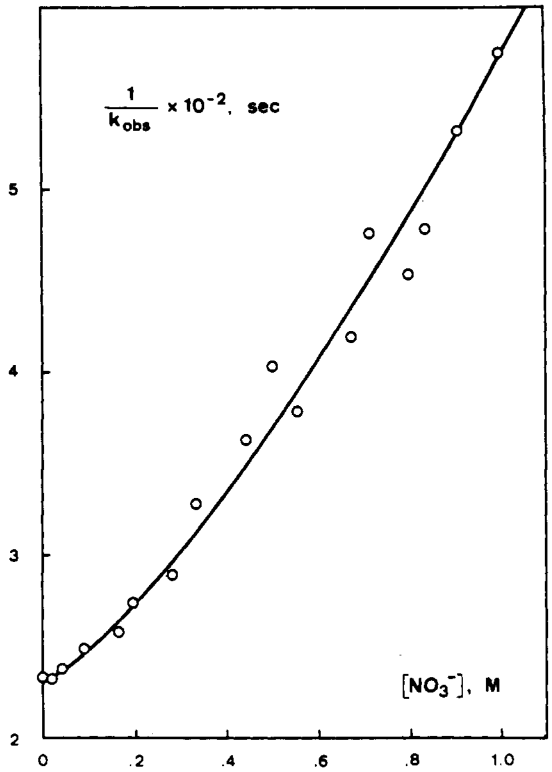

Figure 1. Kinetics of spontaneous cleavage of M^{5+} in NO_3^-/ClO_4^- medium (25 °C, $I = 1.0$). Full line: best fit to rate law 2. The best fit to rate law 1 leads to an extrapolated value of k_{obsd} at $[NO_3^-]$ that is distinctly inferior to k_{obsd} in pure ClO_4^- medium.

Table IV. Fraction of $(H_3N)_5CoSCN^{2+}$ (F_{SCN}) and of $(H_3N)_5CoNCS^{2+}$ (F_{NCS}) in the Spontaneous Cleavage of $[(H_3N)_5CoOHCo(NH_3)_5]^{5+}$ at 25 °C, $I = 1.0$, and pH 3.3

$[NCS^-]$, mol dm^{-3}	F_{SCN}[a]	F_{NCS}[a]	F_{NCS}/F_{SCN}[b]	% recovery
0.25	0.025	0.139	5.6/1	94
0.5	0.050	0.232	4.6/1	97
	0.048	0.156	3.3/1	100
0.75	0.070	0.282	4.0/1	101
1.0	0.093	0.364	3.9/1	98
	0.108	0.290	2.7/1	96

[a] Only one Co-O bond is broken. Data normalized to 100% recovery. [b] Mean value: 4.0/1.

This rate law does not improve the fit for Cl^-, NCS^-, and $CH_3SO_3^-$.[18] However, it offers a slight advantage for NO_3^-. Here, the F test[19] (which becomes more rigorous for increasing numbers of parameters) gave 84% confidence for rate law 2 over rate law 1.

We have therefore sought confirmation for the different behavior attributed to NO_3^- by investigating the kinetics in NO_3^-/NCS^- media. Again, the fit to the more complex rate law

$$k_{obsd} = \frac{k'_0 + k'_{NO_3}K'_{NO_3}[NO_3^-]}{1 + K'_{NO_3}[NO_3^-] + K'_{(NO_3)_2}K'_{NO_3}[NO_3^-]^2} \qquad (3)$$

(where the primed constants refer to NCS^- supporting electrolyte) was superior, within 90% confidence limits, relative to a rate expression analogous to (1) (Tables I and III). Here, the accuracy was better, since the solubility of the mono-ol salts was distinctly higher. A reactive ion pair of M^{5+} with NO_3^- may thus be postulated with more confidence. However, for the following discussion of the product distribution, it is useful to demonstrate that it would not be safe to rule out *reactive* ion aggregates in these cleavage reactions.

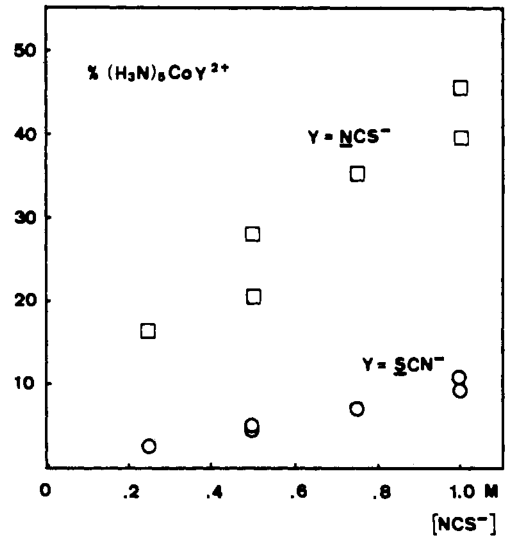

Figure 2. Product distribution for the spontaneous cleavage of M^{5+} in NCS^-/ClO_4^- media: Y = *N*CS$^-$, N-bonded $(H_3N)_5CoNCS^{2+}$; Y = *S*CN, S-bonded isomer.

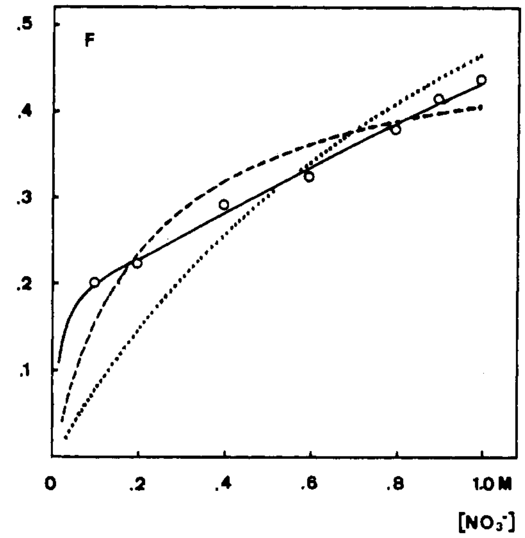

Figure 3. Product distribution function for the spontaneous cleavage of M^{5+} in NO_3^-/ClO_4^- media: best fit to model 1a (···), model 2b-1 or 2b-2 (- - -), and model 2a (—).

Product Analysis. The products of spontaneous cleavage of $[(H_3N)_5CoOHCo(NH_3)_5]^{5+}$ were determined for a series of mixed NCS^-/ClO_4^- electrolytes (Table IV, Figure 2). Ion-exchange chromatography afforded a 2+ fraction ($(H_3N)_5CoNCS^{2+}$ and $(H_3N)_5CoSCN^{2+}$)[20] and $(H_3N)_5CoOH_2^{3+}$. The ratio % $(H_3N)_5CoNCS^{2+}$/% $(H_3N)_5CoSCN^{2+}$ was determined spectrophotometrically.[20,21] This ratio (4.0 ± 1.0) is subject to considerable error from the relative inaccuracy with which the ex-

---

[18] An attempt to fit the Cl^-/ClO_4^-, $CH_3SO_3^-$, or NCS^-/ClO_4^- data to rate law 2 resulted in undetermined parameters.

[19] "Standard Mathematical Tables", 20th ed.; Cranwood Parkway: Cleveland, OH, 1972; pp 591–597.

[20] Buckingham, D. A.; Creaser, I. I.; Sargeson, A. M. *Inorg. Chem.* **1970**, *9*, 655.

[21] The appearance of the S-bonded isomer is in apparent contradiction with a report by Wharton and Sykes,[22] who did not detect any $(H_3N)_5CoSCN^{2+}$ among the cleavage products of the mono-ol cation at pH 1 in the presence of thiocyanate. Under these conditions, the acid-induced cleavage pathway predominates and the corresponding linkage isomer distribution may be different altogether, although this is not very likely. We note, however, that $(H_3N)_5CoSCN^{2+}$ is somewhat unstable in solutions containing HNCS,[23] i.e. under the conditions used in ref 22. We have therefore kept our solutions at pH > 3 during reaction and workup, and a blank experiment on authentic $(H_3N)_5CoSCN^{2+}$ confirmed the absence of detectable S → N rearrangement under these conditions.

[22] Wharton, R. K.; Sykes, A. G. *J. Chem. Soc., Dalton Trans.* **1973**, 439.

[23] Marty, W., unpublished results.

Table V. Fraction of $(H_3N)_5CoONO_2{}^{2+}$ in Spontaneous Cleavage of $[(H_3N)_5CoOHCo(NH_3)_5]^{5+}$ at 25 °C, $I = 1.0$, and pH 3.3

$[NO_3{}^-]$, mol dm^{-3}	F_{obsd}[a]	F_{calcd} model 1a[c]	 model 2a[d]	 model 2b-1[e]	 model 2b-2[f]	% recovery
0.0	0.0[b]	0.0	0.0	0.0	0.015	
0.1	0.203	0.080	0.203	0.157	0.157	97
0.2	0.225	0.148	0.228	0.237	0.235	103
0.4	0.292	0.259	0.281	0.320	0.318	101
0.6	0.324	0.343	0.336	0.362	0.361	98
0.8	0.380	0.411	0.387	0.387	0.388	99
0.9	0.415	0.440	0.410	0.396	0.398	100
1.0	0.437	0.466	0.432	0.404	0.406	98

[a] Only one Co–O bond is broken. Data are normalized to 100% recovery. [b] No nitrato pentaammine can be formed in the absence of $NO_3{}^-$. [c] $R_{M(NO_3)_n} = 0.87$ dm^3 mol^{-1}, $R = 0.15$. Model lab gives very similar values for F_{calcd}, but $R_{MY_n}{}^b = 0.0 \pm 0.1$. [d] $f = 19$ dm^3 mol^{-1}, $R_{M(NO_3)_n} = 8.7$ dm^3 mol^{-1}, $R_{M(NO_3)_{n+1}} = 0.69$ dm^3 mol^{-1}, $R = 0.019$. [e] $c = 4.4$, $R_M = 0$, $R_{MNO_3} = 0.96$, $R = 0.080$. [f] $d/c = 4.16$ dm^3 mol^{-1}, $R_{MNO_3} = 0.015$, $R_{M(NO_3)_2} = 1.0$, $R = 0.077$.

Table VI. Fraction of $(H_3N)_5CoCl^{2+}$ in Spontaneous Cleavage of $[(H_3N)_5CoOHCo(NH_3)_5]^{5+}$ at 25 °C, $I = 1.0$, and pH 3.5

$[Cl^-]$, mol dm^{-3}	F_{obsd}[a]	F_{calcd} model 1a[c]	 model 2a[d]	 model 2b-1[e]	 model 2b-2[f]
0.0	0.0[b]	0.0	0.0	0.0	0.015[g]
0.1	0.186	0.099	0.183	0.147	0.149
0.2	0.234	0.181	0.242	0.241	0.238
0.4	0.330	0.306	0.326	0.352	0.347
0.6	0.406	0.398	0.395	0.416	0.412
0.8	0.440	0.469	0.453	0.458	0.455
0.9	0.490	0.498	0.478	0.474	0.471
1.0	0.474/0.520	0.524	0.501	0.487	0.486

[a] Only one Co–O bond is broken. Results are taken from ref 15. [b] No chloro pentaammine can be formed in the absence of Cl^-. [c] $R_{MCl_n} = 1.10$ dm^3 mol^{-1}, $R = 0.085$. Model 1ab gives very similar values for F_{calcd}, but $R_{MY_n}{}^b = 0.0 \pm 0.1$. [d] $f = 14.3$ dm^3 mol^{-1}, $R_{MCl_n} = 4.8$ dm^3 mol^{-1}, $R_{MCl_{n+1}} = 0.92$ dm^3 mol^{-1}, $R = 0.031$. [e] $c = 2.9$, $R_M = 0$, $R_{MCl} = 1.9$, $R = 0.051$. [f] $d/c = 2.6$ dm^3 mol^{-1}, $R_{MCl} = 0.015$, $R_{MCl_2} = 2.0$, $R = 0.047$. [g] Value excluded from the calculation of R.

tinction coefficient at the isosbestic point could be determined. The variation of the ratio bears no obvious relation with $[NCS^-]$. Unexpectedly, these ratios are quite different from those found for alkaline hydrolysis[20] (~0.3) and for the nitrosation of azidopentaammines (~0.3).[20,24]

The cleavage products in $NO_3{}^-/ClO_4{}^-$ media at pH 3.0–3.5 were $(H_3N)_5CoNO_3{}^{2+}$ and $(H_3N)_5CoOH_2{}^{3+}$ (Table V, Figure 3). As in the $NCS^-/ClO_4{}^-$ media, the aniono complex is formed much faster than by subsequent anion substitution in $(H_3N)_5CoOH_2{}^{3+}$, and it must arise during the act of cleavage of the mono-ol. The amount of $(H_3N)_5CoONO_2{}^{2+}$ increases nonlinearly with increasing $[NO_3{}^-]$, a phenomenon similar to that observed for the $NCS^-/ClO_4{}^-$ and the previously investigated[15] $Cl^-/ClO_4{}^-$ media (Table VI, Figure 4).

Discussion

Product Analysis. In previous work,[15] the products of spontaneous cleavage of M^{5+} in $Cl^-/ClO_4{}^-$ media, viz. $(H_3N)_5CoCl^{2+}$ and $(H_3N)_5CoOH_2{}^{3+}$, were quantitatively determined as a function of $[Cl^-]$. It was noted[15] that more $(H_3N)_5CoCl^{2+}$ was found than expected on the basis of the observed, simple kinetics (rate law 1) and of a coordinatively unsaturated intermediate with known scavenging properties. Nevertheless, no models for the product-determining step(s) were proposed, and it is the purpose of this paper to present a more detailed discussion of this mechanistically significant aspect. The discussion will include the above data ($Y^- = Cl^-$),[15] as well as newly determined data for $Y^- = NO_3{}^-$. We will use the following notation: CoY for $(H_3N)_5CoY^{2+}$, $CoOH_2$ for $(H_3N)_5CoOH_2{}^{3+}$, and $M{\cdot}Y_n$ for $[(H_3N)_5CoOHCo(NH_3)_5]{\cdot}Y_n{}^{(5-n)+}$ (ion aggregates of M^{5+} with n anions Y^-). The product distribution function, $F([Y]) = [CoY]_\infty/[M]_0$ ($Y = NO_3{}^-$, Cl^-; Tables V and VI), depends on the number and nature of the intermediates as well as on the mechanism and has been analyzed in terms of several models for product formation.

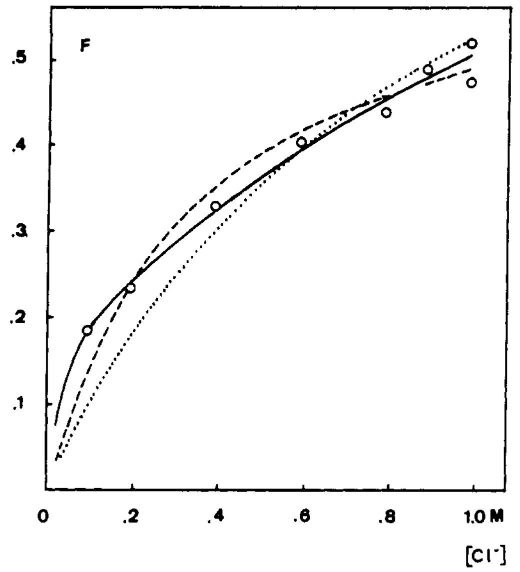

Figure 4. Product distribution function for the spontaneous cleavage of M^{5+} in $Cl^-/ClO_4{}^-$ media: best fit to model 1a (···), model 2b-1 or 2b-2 (- -), and model 2a (—).

Our models for product formation differ in the number of reactive species considered. First, only one species, e.g. M or M·Y, could lead to CoY. The corresponding models shall be given a symbol starting with the number 1. Alternatively, two species, e.g. M and M·Y or M·Y and $M{\cdot}Y_2$, could lead to CoY in parallel pathways. The corresponding symbols shall begin by the number 2. Models with more than two reactive species are inconsistent with all kinetic data, unless the rate laws are deceptively simple (see below).[25] Thus, the number of reactive species is not limited a priori or by undisputable experimental evidence. We are therefore left with the pragmatic approach to search for the *model implying the smallest possible number of reactive species* that leads to a satisfactory fit, consistent with the experimental precision.

Anions Y can be scavenged from solution, or they can enter the first coordination sphere while already dwelling in the second

---

(24) Buckingham, D. A.; Creaser, I. I.; Marty, W.; Sargeson, A. M. *Inorg. Chem.* **1972**, *11*, 2738.

(25) A rate law of the form (2) may reduce to the simpler form (1), if numerator and denominator accidentally contain a common factor:

$$k_{obsd} = \frac{k_0 + k_Y K_Y[Y]}{1 + K_Y[Y] + K_Y K_{Y_2}[Y]^2} = \frac{k_0(1 + b[Y])}{(1 + a[Y])(1 + b[Y])} = \frac{k_0}{1 + a[Y]}$$

where $k_Y = bk_0/(a + b)$, $K_Y = a + b$, and $K_{Y_2} = ab/(a + b)$. By analogy, a rate law with three reactive species (free mono-ol, ion pair, and ion triplet) could lead to accidental cancellation of two factors in the numerator by two out of three denominator factors:

$$k_{obsd} = \frac{k_0 + k_Y K_Y[Y] + k_{Y_2} K_{Y_2} K_Y[Y]^2}{1 + K_Y[Y] + K_{Y_2} K_Y[Y]^2 + K_{Y_3} K_{Y_2} K_Y[Y]^3} = \frac{k_0(1 + b[Y])(1 + c[Y])}{(1 + a[Y])(1 + b[Y])(1 + c[Y])} = \frac{k_0}{1 + a[Y]}$$

where $k_Y = k_0(b + c)/(a + b + c)$, $k_{Y_2} = k_0bc/(ab + bc + ac)$, $K_Y = a + b + c$, $K_{Y_2} = (ab + bc + ac)/(a + b + c)$, and $K_{Y_3} = abc/(ab + bc + ac)$.

Scheme II. Summary of Potential Cleavage Pathways for the Mono-ol Cation, Where $MY_n{}^*$ Are Coordinatively Unsaturated, Steady-State Intermediates

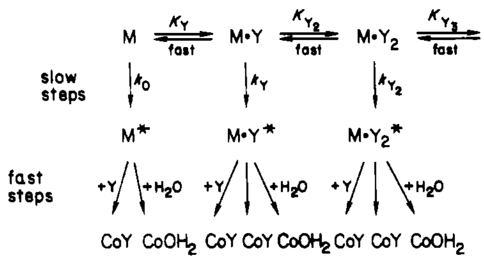

sphere. The first is an intermolecular reaction, and its rate law is $d[CoY]/dt = k_Y{}^{a,MY_n}[MY_n{}^*][Y^-]$ ($n = 0, 1, ...$; the asterisk denotes the dissociatively activated, reactive species; see below). Models considering this mode of product formation will be symbolized by the letter a. If the entering anion Y is captured from the second coordination sphere, the rate law of this intramolecular step is $d[CoY]/dt = k_Y{}^{b,MY_n}[MY_n{}^*]$ ($n = 1, 2, ...$), and these mechanisms will be designated by the letter b. For a given number ($\geqslant 2$) of reactive species there are many possible combinations of individual steps of type a or b.

Before presenting the individual models, we wish to point out one serious limitation. The shape of the product distribution functions $F([Y^-])$ cannot generally be analyzed in terms of absolute numbers (n) of associated anions in the reactive ion aggregates $M{\cdot}Y_n$. This arises from the present practical impossibility of determining product distributions at very low $[Y^-]$. However, the *relative* numbers of anions in a pair of reactive species and also the reaction order with respect to $[Y^-]$ (=0 or 1) can be determined.

The final product distribution functions $F([Y])$ characteristic of each model are obtained by integrating the differential rate law of product formation at $t \to \infty$. All possible models can be treated as particular cases within Scheme II. The consistency of this scheme with the kinetics will be examined in the following section. Different models for product formation can be derived depending on the relative reactivities of $M{\cdot}Y_n$ ($n = 0, 1, 2, ...$) and on the reactivity of $M{\cdot}Y_n{}^*$ with Y from solution and from the second coordination sphere, respectively.

Models with One Reactive Species. If only one reactive species is assumed, then there are two principal possibilities: models 1a and 1ab. Model 1a allows for the intermolecular pathway $k_Y{}^{a,MY_n}$ only, whereas in model 1ab the intramolecular pathway $k_Y{}^{b,MY_n}$ (scavenging from the second coordination sphere) is considered simultaneously, along with $k_Y{}^{a,MY_n}$. None of these models leads to an acceptable fit (Tables V and VI).

model 1a

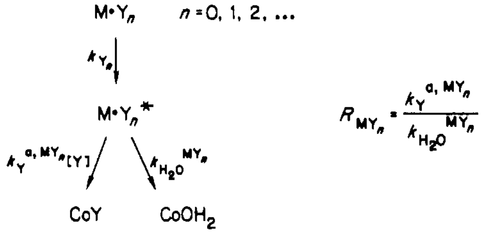

$$R_{MY_n} = \frac{k_Y{}^{a,MY_n}}{k_{H_2O}{}^{MY_n}}$$

$$F([Y]) = [Y]/([Y] + R_{MY_n}{}^{-1})$$

model 1ab

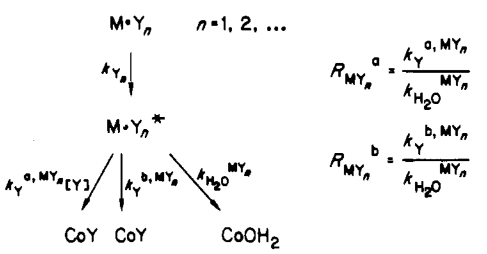

$$R_{MY_n}{}^{a} = \frac{k_Y{}^{a,MY_n}}{k_{H_2O}{}^{MY_n}} \qquad R_{MY_n}{}^{b} = \frac{k_Y{}^{b,MY_n}}{k_{H_2O}{}^{MY_n}}$$

$$F([Y]) = \frac{[Y] + \left(R_{MY_n}{}^{a}\right)^{-1}\left(R_{MY_n}{}^{b}\right)}{[Y] + \left(R_{MY_n}{}^{a}\right)^{-1}\left(R_{MY_n}{}^{b}\right) + \left(R_{MY_n}{}^{a}\right)^{-1}}$$

A third model (model 1b), where scavenging of Y occurs exclusively from the second coordination sphere (through an intramolecular process), would lead to $[CoY]_{t\to\infty}$ independent from [Y]. This is at variance with the results (Table IV) and will not be discussed further.

model 1b

$$F([Y]) = 1/(1 + (R_{MY_n}{}^{b})^{-1})$$

Models Involving More Than One Reactive Species. If we allow for several reactive species that are related to each other by addition or loss of one associated anion in a preequilibrium, we have Scheme III ($n = 0, 1, 2, ...$). If scavenging of Y is intermolecular, only the $k_Y{}^{a}$ pathways contribute to the formation of CoY and expression 4 for the product distribution functions is obtained.

$$F([Y])_a = \frac{[Y]}{1 + c[Y] + d[Y]^2 + ...}\left(\frac{1}{[Y] + (R_{MY_n}{}^{a})^{-1}} + \frac{c[Y]}{[Y] + (R_{MY_{n+1}}{}^{a})^{-1}} + \frac{d[Y]^2}{[Y] + (R_{MY_{n+2}}{}^{a})^{-1}} + ...\right) \quad (4)$$

$$c = k_{Y_{n+1}}K_{Y_{n+1}}/k_n \qquad d = k_{Y_{n+2}}K_{Y_{n+2}}K_{n+1}/k_n$$

Another product formation scheme can be envisaged, where ion aggregates $M{\cdot}Y_n$ ($n = 1, 2, ...$) are reactive and form CoY by an *intra*molecular pathway. However, at least at low [Y], free M must also be present, and if it forms CoY, then the species M* must capture Y exclusively by an intermolecular pathway. Thus, in Scheme III, $M{\cdot}Y_n = M$, $M{\cdot}Y_n{}^* = M^*$, $M{\cdot}Y_{n+1} = M{\cdot}Y$, etc. For M*, the rate constant of *intra*molecular reaction with Y is zero, whereas for all anion aggregates $M{\cdot}Y$, $M{\cdot}Y_2$, ..., the rate constants of *inter*molecular reaction are zero. The corresponding product distribution function is shown in (5), parameters c and d being defined as in (4).

$$F([Y])_{a,b} = \frac{[Y]}{1 + c[Y] + d[Y]^2 + ...}\left(\frac{1}{[Y] + R_M{}^{-1}} + \frac{c}{1 + (R_{MY}{}^{b})^{-1}} + \frac{d[Y]}{1 + (R_{MY_2}{}^{b})^{-1}} + ...\right) \quad (5)$$

Formulas 4 and 5 have been derived by assuming an ion aggregation preequilibrium situation and steady-state concentrations of the reactive species, M*, MY*, ..., $MY_n{}^*$.

In formulas 4 and 5, the factor $[Y]/(1 + c[Y] + d[Y]^2 + ...)$ expresses the influence of the relative rates of formation of the reactive intermediates on the product distribution; it is common to models a and b. The terms in large parentheses describe, one by one, the product-determining steps of all reactive intermediate states.

From the general expressions (4) and (5), limiting expressions can be derived, depending on the relative magnitude of the various terms in the factor $[Y]/(1 + c[Y] + d[Y]^2 + ...)$.[26] If all but one $M{\cdot}Y_n$ species are either very unstable or much less reactive than the others, or both, then eq 4 reduces to the expression for model 1a (see above). In particular, if for $n = 0$, $1 >> c[Y]$, $d[Y]^2$, then M^{5+} is the only product-forming species, or if for $n = 1$, $c[Y] >> 1$, $d[Y]^2$, then M·Y is the only product-forming species, etc.

---

(26) The values of R_{MY_n} cannot influence the magnitude of $F([Y])$ independently from the parameters c, d, ..., for kinetically unimportant pathways cannot affect the product distribution functions, even if the corresponding R_{MY_n} values are quite large.

Scheme III. Product Formation Pathways ($n = 0, 1, 2, \ldots$)

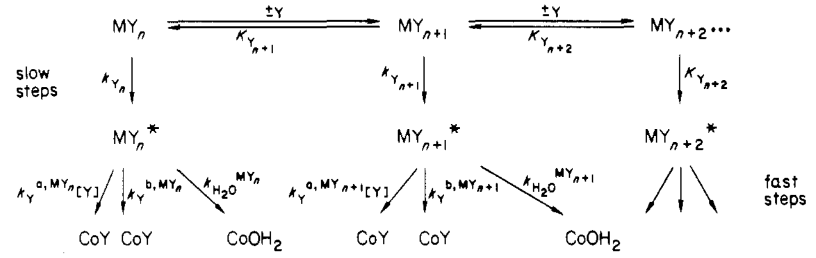

If *two* species, M·Y$_n$* and M·Y$_{n+1}$*, are assumed to form products via an intermolecular pathway, then the expression given in model 2a applies, provided $1 + c[Y] >> d[Y]^2$ (for $n = 0, f = c$) or $c[Y] + d[Y]^2 >> 1$ (for $n = 1$ and $f = d/c$). In model 2a, *two* reactive species, differing in composition by one associated anion, scavenge Y from the *bulk solution*. However, from the shape of the product distribution curve alone, it cannot be said what the absolute composition of the two species is; M and M·Y, M·Y and M·Y$_2$, etc. may be the product-forming species.

model 2a

$$F([Y])_a = \frac{[Y]}{1 + f[Y]}\left(\frac{1}{[Y] + (R_{MY_n}{}^{a})^{-1}} + \frac{f[Y]}{[Y] + (R_{MY_{n+1}}{}^{a})^{-1}}\right)$$

Similarly, eq 5 may reduce to one of the expressions for one-particle models (see above). Thus, for $n = 0$ and $1 >> c[Y]$, $d[Y]^2$, (5) reduces to the formula for model 1a. If $c[Y] >> 1$, $d[Y]^2$ (for $n = 1$) or $d[Y]^2 >> 1$, $c[Y]$ (for $n = 2$), eq 5 simplifies to the expression for model 1b.

If *two* reactive species are involved, and if product formation is intramolecular, wherever possible, then eq 5 may reduce to one of two different expressions: (i) If M and M·Y are reactive, then scavenging of Y by M* is intermolecular, but M·Y* reacts via an intramolecular pathway. Thus, if $1 + c[Y] >> d[Y]^2$, eq 5 reduces to the expression shown in model 2b-1. (ii) If both product-forming species are ion aggregates (M·Y$_n$* and M·Y$_{n+1}$*, $n = 1, 2, \ldots$), product formation is exclusively intramolecular. For $c[Y] + d[Y]^2 >> 1$, eq 5 reduces to the expression shown in model 2b-2, where, e.g., for $n = 1, f = d/c$, etc. Again, n remains generally unknown from analysis of $F([Y])$.

model 2b-1

$$F([Y])_b = \frac{[Y]}{1 + c[Y]}\left(\frac{1}{[Y] + R_M{}^{-1}} + \frac{c}{1 + R_{MY}{}^{-1}}\right)$$

model 2b-2

$$F([Y])_b = \frac{1}{1 + f[Y]}\left(\frac{1}{1 + R_{MY_n}{}^{-1}} + \frac{f[Y^-]}{1 + R_{MY_{n+1}}{}^{-1}}\right)$$

The data have been fitted to models 1a, 1ab, 2a, 2b-1, and 2b-2 (Tables V and VI).[27] Clearly, model 2a gives the best fit for $Y^- = Cl^-$ and NO_3^- (Figures 3 and 4). Furthermore, in model 2b-1, $R_M \simeq 0$ for both Cl^- and NO_3^-, and it is difficult to see why M* should not give any CoY if it is assumed to be reactive. The values $R_{MY}{}^b \simeq 0.015$ in model 2b-2 (for a 4+ charged species) and $R_{MY_n}{}^b \simeq 0$ in model 1ab, for Cl^- and NO_3^- also appear unreasonably small, as scavenging from the second sphere might be expected to be quite efficient. Existing literature R data for 4+ charged species are much higher (see below), and this also argues against model 2b-2.[28]

The distinction between M* and M·Y* from M·Y* and M·Y$_2$* in model 2a as the product-forming intermediate states can be attempted by comparing the R values with those for other reactions. For the scavenging of NO_3^- in the Hg^{2+}-induced aquation of $(H_3N)_5CoCl^{2+}$ (where $(H_3N)_5CoCl{\cdot}Hg^{4+}$ is involved), the mechanistic equivalent of model 2a-2 gave $R = 1.06$ dm^3 mol^{-1}.[2] Similarly, azide scavenging by the 4+ charged, reactive intermediate in the base-catalyzed cleavage of the (±)-*cis,cis*-$(en)_2NH_3CoNH_2CoNH_3(en)_2{}^{5+}$ dimer gave $R_{N_3} = 0.61$ dm^3 mol^{-1}.[29]

For the reactive, 4+ charged mono-ol species M·Y*, the R values (model 2a) are similar for $Y^- = Cl^-$, NO_3^-: $R_{MCl} = 0.92$ dm^3 mol^{-1} and $R_{MNO_3} = 0.69$ dm^3 mol^{-1}. They resemble the above literature values. For the unassociated mono-ol, $R_M = 4.8$ dm^3 mol^{-1} in Cl^-/ClO_4^- and $R_M = 8.7$ dm^3 mol^{-1} in NO_3^-/ClO_4^-. There appears to exist no comparison in the literature for these last two figures. In conclusion, this comparison supports M* and MY* as the reactive species.[30]

The main result of this study is quite unequivocal: the reacting mono-ol species scavenge nucleophiles from the bulk solution and not from the second coordination sphere. This result may be disappointing to partisans of an I_d mechanism for spontaneous aquation of cobalt(III) pentaammines. On the other hand, the high selectivity for anions (relative to neutral ligands) may be disturbing to adherents of a stepwise (D) mechanism. However, the positively charged, bulky leaving group, $(H_3N)_5CoOH^{2+}$ is likely to exert some influence on a possible coordinatively unsaturated intermediate through its relatively slow diffusion from the center of reaction and by its ionic atmosphere. The effect of the ionic atmosphere can explain the much more efficient anion scavenging compared with more lowly charged substrates with fast leaving groups (1.3–3.3% $(H_3N)_5CoCl^{2+}$ in HCl (1 mol dm^{-3}),[10] against 48% for the mono-ol in NaCl (1 mol dm^{-3})). Again, this difference is not due to scavenging of nucleophiles from

---

[27] Combinations between models 2a and 2b (simultaneous scavenging from the second sphere and from solution, either by the same or by different reactive intermediate states) do not lead to significant new cases. The first case has been discussed, and the second is tantamount to model 2b-1 with M* and MY* as the reactive species. Thus, all significant two-species models have been examined.

[28] One reviewer has proposed the following, alternative intramolecular reaction scheme for CoY formation:

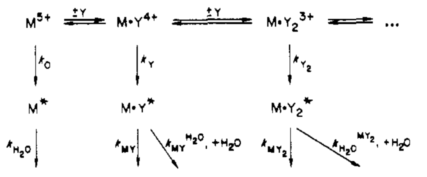

Here, the intermolecular scavenging of Y by M* is ruled out a priori. The corresponding product distribution function corresponds to eq 5 with $R_M \rightarrow 0$:

$$F([Y]) = \frac{[Y]}{1 + c[Y] + d[Y]^2 + \ldots}\left(\frac{c}{1 + R_{MY}{}^{-1}} + \frac{d[Y]}{1 + R_{MY_2}{}^{-1}} + \ldots\right)$$

This analysis suffers from the impossibility of examining whether such intermolecular scavenging does exist or not. Our model 2b-1 leaves this possibility open; in fact, the best fit to this particular model leads to $R_M \simeq 0$. At any rate, this additional model does not lead to a better fit than model 2a at a two-species level.

[29] Rotzinger, F. P.; Marty, W. *Inorg. Chem.* **1983**, *22*, 3593.

[30] This is also supported by the rate data, where k_0, the rate constant of unassociated M^{5+}, makes a considerable contribution at all [Y] studied.

the second coordination sphere in the mono-ol. In this context, the observed preference for N-bonded thiocyanate is of interest. In previous cases, a preference for the S end was found and interpreted by a very short lifetime of the five-coordinate intermediate, where desolvation of SCN^- was the rate-determining step in product formation. In the case of the mono-ol, it appears that the intermediate state lifetime is sufficiently long for developing a distinct selectivity.

The possible participation of the ClO_4^- inert electrolyte anion in product formation deserves attention. Perchlorate ion may be captured during the cleavage process, giving rise to formation of known[11] $(H_3N)_5CoOClO_3^{2+}$ ion. This species is very reactive and some anion competition occurs during its spontaneous aquation.[11] The efficiency of ClO_4^- capture during cleavage of the mono-ol cation is not presently known, but the capture of NO_3^- (F_{obsd} = 0.437 in 1 M NO_3^-) or of Cl^- (F_{obsd} = 0.497 in 1 M Cl^-) may provide a reasonable estimate. The extent of capture of Cl^- in spontaneous aquation of $(H_3N)_5CoOClO_3^{2+}$ is known to be small (3% $(H_3N)_5CoCl^{2+}$ in 1 M HCl).[11] Thus, only <1.5% of the $(H_3N)_5CoCl^{2+}$ ions are expected to arise from ClO_4^- capture in mono-ol cleavage and subsequent Cl^- capture in $(H_3N)_5CoOClO_3^{2+}$ aquation. Analogous data for NO_3^- are not available, but the fact that $F([Y])$ values for Y = Cl^-, NO_3^- are qualitatively analogous and quantitatively similar argues against a major involvement of ClO_4^- capture in the formation of $(H_3N)_5CoONO_2^{2+}$ and $(H_3N)_5CoCl^{2+}$ in the cleavage of the mono-ol cation in NO_3^- or Cl^- media.

Kinetics. The rate data (Tables I–III) are accommodated by Scheme II, where consecutive ion aggregation preequilibria are involved. For Y = NO_3^-, in ClO_4^- and in NCS^- media, the k_Y path makes a small contribution (Tables I and IIIb) that is near the limit of detection, due, in part, to experimental difficulties. No k_Y path is detected for NCS^-, Cl^-,[15] and $CH_3SO_3^-$[15] in ClO_4^- medium (rate law 1; Tables I and IIIa), at least for the spontaneous-cleavage data alone.

The data were analyzed in terms of an approximation, where possible ion association with the supporting electrolyte (ClO_4^- or NCS^-) is assumed to be constant. However, Y^- most likely competes with ClO_4^- or NCS^- in aggregate formation, and $[ClO_4^-]$ and $[NCS^-]$ vary within as wide limits as $[Y^-]$. Thus, K_Y and K_{Y_2} do *not* simply correspond to equilibrium constants of the type represented in

$$[(H_3N)_5CoOHCo(NH_3)_5{\cdot}(ClO_4)_n]^{(5-n)+} + Y^- \overset{K_Y}{\rightleftharpoons} [(H_3N)_5CoOHCo(NH_3)_5{\cdot}Y{\cdot}(ClO_4)_{n-1}]^{(5-n)+} + ClO_4^-$$

(n = 1, 2, ...; several species with different values of n are possibly coexisting), since one Y^- may replace more than one ClO_4^- or vice versa. Only the kinetics at $[Y^-] < 0.1$ mol dm^{-3} are uninfluenced to an acceptable approximation by the variation of $[ClO_4^-]$. In this range, however, the ion aggregation effect on the rate is too small for a proper determination of the rate law. The data in the range $[Y^-]$ = 0–1 mol dm^{-3} may thus result in a mechanistically misleading rate expression. A deceptively simple or a spuriously complex rate law may arise from the simultaneous variation of $[Y^-]$ and $[ClO_4^-]$. For Y^- = Cl^-, $CH_3SO_3^-$, and NCS^- in ClO_4^- medium, the observed rate law is likely to be deceptively simple.[25] For NO_3^-, the more complex rate law (which may still be deceptively simple) obtains.

For the mono-ol cation, the values of K_Y increase in the order Y^- = Cl^- < NO_3^-. Systematic studies on ion-pair formation constants of cobalt(III) ammine species do not include 5+ charged cations. However, data on $[(H_3N)_5CoX]Y_2$ (X = $RCOO^-$, R = alkyl) at high ionic strength show that the order of stability of aggregates with different anions Y varies little with X. The stabilities increase in the order $Cl^- < Br^- < I^- < NO_3^-$, i.e. inversely to the expected order of electrostatic interaction.[31] The sequence $Cl^- < NO_3^-$ is also found in the mono-ol. There, at least the consecutive ion-pairing constants, $K_{NO_3} > K_{(NO_3)_2}$ are in keeping with electrostatically controlled ion aggregation. The absolute values of K_Y (and K_{Y_2}) turn out to be much smaller than anticipated for a 5+ charged ion, and undoubtedly this is due to competing ion aggregate formation with supporting ClO_4^- or NCS^-.

Despite obvious ambiguities, the kinetic data give a qualitative overall view of the mechanistically important species and pathways. The results are in qualitative agreement with the more straightforward, independent analysis from the product distribution functions, at least in the case of Y^- = NO_3^-. Thus, both M^{5+} and $M{\cdot}NO_3^{4+}$ (or, less likely, a homologous pair of higher ion aggregates) were found to be reactive in the kinetics as well as from the product distribution function. The close analogy between the product distribution functions for Y^- = NO_3^- and Cl^- leads us to believe that the rate law for Y^- = Cl^- is deceptively simple.

Experimental Part

Materials. $[(H_3N)_5CoOHCo(NH_3)_5]Cl_5{\cdot}H_2O$ was prepared[14,15] and checked for purity as described. The chloride salt was precipitated three times with saturated $NaNO_3$ in 2% acetic acid to give $[(H_3N)_5CoOHCo(NH_3)_5](NO_3)_5$ free of Cl^- and $[(H_3N)_5CoONO_2](NO_3)_2$. All other chemicals were reagent grade quality (Fluka or Merck) and were used as received. Deionized water was distilled before use. Electrolyte solutions ($NaClO_4$, $NaNO_3$, NaNCS) were filtered through Millipore membrane filters before use.

Kinetics. Kinetics and product spectra were measured on a Varian Techtron 635 spectrophotometer. For the kinetics studies, 0.5–2 mg of $[(H_3N)_5CoOHCo(NH_3)_5](NO_3)_5$ was dissolved in dilute $HClO_4$ (10 cm^3, pH 3.3) and mixed with the appropriate electrolyte of twice the final concentration. The prethermostated mixture was then transferred into a thermostated quartz cell (5 or 10 cm) in the spectrophotometer.

Product Analysis. $[(H_3N)_5CoOHCo(NH_3)_5](NO_3)_5$ (8–35 mg) was dissolved within less than 20 s in dilute $HClO_4$ (10 or 50 cm^3, pH 3.5), and an equal volume of a solution of $NaNO_3/NaClO_4$ of twice the final concentration was added at once. A fraction of the mono-ol salt crystallized. The reaction was carried out in heterogeneous suspension (25 °C, stirring) for 1–3 h. The reaction mixture was then diluted fivefold and adsorbed on to Dowex 50W-X2, 200–400 mesh in the H^+ form. $HClO_4$ (1 mol dm^{-3}) eluted $(H_3N)_5CoONO_2^{2+}$ (ϵ_{502} = 56.3 dm^3 mol^{-1} cm^{-1}), and H_2SO_4 (2 mol dm^{-3}) eluted $(H_3N)_5CoOH_2^{3+}$ (ϵ_{492} = 47.7 dm^3 mol^{-1} cm^{-1}).[32] The fractions were analyzed spectrophotometrically, and a small correction for aquation of $(H_3N)_5CoONO_2^{2+}$ during reaction and workup was made by using $k = 2.4 \times 10^{-5}$ s^{-1} (I = 0.12, 25 °C).[33]

$[(H_3N)_5CoOHCo(NH_3)_5]Cl_5{\cdot}H_2O$ (46–60 mg) was dissolved directly in 20 cm^3 of $NaNCS/NaClO_4$ (pH 3.5, $HClO_4$, I = 1.0, 25 °C). After ca. 10 half-lives, the reaction mixture was diluted fivefold and adsorbed onto Dowex as above. $HClO_4$ (1 mol dm^{-3}) eluted the mixture of $(H_3N)_5CoNCS^{2+}$ and $(H_3N)_5CoSCN^{2+}$. The sum of the two was determined by measuring the optical density at their isosbestic point (ϵ_{555} = 55 dm^3 mol^{-1} cm^{-1}). The two components were determined by using ϵ_{288}^{SCN} = 15 600, ϵ_{288}^{NCS} = 1232, ϵ_{512}^{NCS} = 161, and ϵ_{512}^{SCN} = 74 (all in dm^3 mol^{-1} cm^{-1}).[20] $(H_3N)_5CoOH_2^{3+}$ was eluted and determined as above.

Curve-Fitting Procedures. For the rate data and for the product distribution functions, the calculated parameters were obtained by a nonlinear least-squares procedure where the expression $\sum_{i=1}^{N}[f_i^{obsd} - f(\beta_k,x_i)]^2$ was minimized. In the expression, f_i^{obsd} are measured values of the functions, $f(\beta_k,x_i)$ are calculated values of the functions, where β_k are the function's parameters, or estimates thereof, and x_i are the variables. The calculations were done with use of a locally written program.

Acknowledgment. This work was supported by ETH funds administered through the Betriebsdirektion/Forschungskommission ETH (Grant 10146/41.0415.5). We thank Prof. D. A. Buckingham and Prof. W. G. Jackson for valuable comments on the manuscript.

Registry No. $[(H_3N)_5CoOHCo(NH_3)_5]^{5+}$, 38467-75-3; NO_3^-, 14797-55-8; NCS^-, 302-04-5; ClO_4^-, 14797-73-0; Cl^-, 16887-00-6.

---

(31) Masterton, W. L.; Scola, J. A. *J. Phys. Chem.* **1964**, *68*, 14. Berka, L. H.; Masterton, W. L. *Ibid.* **1966**, *70*, 1641.

(32) Buckingham, D. A.; Olsen, I. I.; Sargeson, A. M.; Satrapa, H. *Inorg. Chem.* **1967**, *6*, 1027.

(33) Jones, W. E.; Jordan, R. B.; Swaddle, T. W. *Inorg. Chem.* **1969**, *8*, 2504.